Emergent Weyl Fermion Excitations in TaP Explored by ^{181}Ta Quadrupole Resonance

H. Yasuoka,[1,2] T. Kubo,[1,3] Y. Kishimoto,[1,3] D. Kasinathan,[1] M. Schmidt,[1] B. Yan,[1] Y. Zhang,[1,4] H. Tou,[3] C. Felser,[1] A. P. Mackenzie,[1,5] and M. Baenitz[1,*]

[1]*Max Planck Institute for Chemical Physics of Solids, 01187 Dresden, Germany*
[2]*Advanced Science Research Center, Japan Atomic Energy Agency, Tokai, Ibaraki 319-1195, Japan*
[3]*Department of Physics, Graduate School of Science, Kobe University, 1-1 Rokkodai, Nada-ku, Kobe 657-8501 Japan*
[4]*IFW Dresden, P.O. Box 270116, 01171 Dresden, Germany*
[5]*SUPA, School of Physics and Astronomy, University of St. Andrews, North Haugh, St. Andrews KY16 9SS, United Kingdom*

(Received 22 November 2016; published 9 June 2017)

The ^{181}Ta quadrupole resonance [nuclear quadrupole resonance (NQR)] technique is utilized to investigate the microscopic magnetic properties of the Weyl semimetal TaP. We find three zero-field NQR signals associated with the transition between the quadrupole split levels for Ta with $I = 7/2$ nuclear spin. A quadrupole coupling constant, $\nu_Q = 19.250$ MHz, and an asymmetric parameter of the electric field gradient, $\eta = 0.423$, are extracted, in good agreement with band structure calculations. In order to examine the magnetic excitations, the temperature dependence of the spin-lattice relaxation rate $(1/T_1T)$ is measured for the f_2 line ($\pm 5/2 \leftrightarrow \pm 3/2$ transition). We find that there exist two regimes with quite different relaxation processes. Above $T^* \approx 30$ K, a pronounced $(1/T_1T) \propto T^2$ behavior is found, which is attributed to the magnetic excitations at the Weyl nodes with temperature-dependent orbital hyperfine coupling. Below T^*, the relaxation is mainly governed by a Korringa process with $1/T_1T = \text{const}$, accompanied by an additional $T^{-1/2}$-type dependence to fit our experimental data. We show that Ta NQR is a novel probe for the bulk Weyl fermions and their excitations.

DOI: 10.1103/PhysRevLett.118.236403

The past decade has seen an explosion of interest in the role of topology in condensed matter physics. Major discoveries have included two-dimensional graphene [1] and the topological insulators (e.g., HgTe or Bi_2Se_3) [2–4], whose topological properties require the existence of gapless surface states. Many of the new materials host exotic excitations whose observation can be regarded as direct experimental evidence for the existence of quasiparticles. Arguably, the most topical of the new classes of materials are Dirac and Weyl semimetals, which are predicted to host topologically protected states in the bulk [5]. In Dirac semimetals [5–7] (e.g., Cd_2As_3 or Na_3Bi), each node contains fermions of two opposite chiralities, whereas in the Weyl semimetals (WSM) [8–12], an even more interesting situation arises. A combination of noncentrosymmetric crystal structure and sizable spin-orbit coupling (SOC) causes the nodes to split into pairs of opposite chirality (Weyl points). In the ideal case, there would be exactly half filling of the relevant bands, such that the Weyl points would sit at the Fermi level (E_F) and the Weyl fermions would be massless. In actuality, in Weyl semimetals such as the d-electron monophosphides NbP and TaP, E_F does not exactly coincide with the Weyl nodes [9,10,12]. However, if the nodes sit close enough to E_F, in a region of linear dispersion ($E \propto k$), the Weyl physics can still be observed in the excitations in the energy window k_BT. A key issue in the study of the monophosphides is therefore to establish how close to the Fermi level the Weyl points sit and to estimate the range of energy over which the linear dispersion exists. This presents a considerable experimental challenge. The nodes appear in the electronic structure of the bulk, and the materials are fully three-dimensional, so the surface-sensitive techniques that have yielded immense insight into other topological physics are not ideally suited to studying the Weyl points. Primarily, one would like to identify a bulk probe that can excite the Weyl fermions and probe the linear dispersion $E \propto k$ indirectly via its energy dependence of the density of states around the Fermi level, which is $N(E) \propto E^2$ for a Weyl node [5]. The magnetic resonance method, in general, has the ability to probe $N(E)$ and was applied successfully to systems like unconventional superconductors (e.g., UPt_3) [13–16] or correlated magnetic semimetals [17] (e.g., SmB_6 [18] or $CeRu_4Sn_6$ [19]). In particular, for unconventional superconductors, the nuclear quadrupole resonance (NQR) spin-lattice relaxation provides information about $N(E)$ around the E_F and allows us to distinguish between point nodes $[N(E) \propto E^2]$ and line nodes $[N(E) \propto E]$ [16]. Therefore, NQR should be a good tool to study the low-energy spin excitations in a Weyl semimetal and is the focus of our presented work (for NMR on topological systems, in general, and for Ta NQR, in particular, see Supplemental Material [20], which includes Refs. [21–26]). Assuming that some of the Weyl points are energetically not too far from E_F, NQR can probe the magnetic excitations of emergent Weyl fermions via the

temperature dependence of the spin-lattice relaxation rate $(1/T_1T)$. Furthermore, a characteristic temperature dependence of the hyperfine coupling between the nuclear spin and electric orbitals near the Weyl nodes has theoretically been predicted which modifies the temperature dependence of $(1/T_1T)$ in a special manner [27]. In fact, TaP has been known to have two sets of Weyl nodes, one located 41 meV (476 K) below E_F and the other is located 13 meV (151 K) above E_F [12]. Accordingly, for temperatures coinciding with the Weyl nodes, excitations associated with the Weyl fermions are expected. Here, we present such characteristic excitations via Ta NQR experiments and explore the emergent Weyl fermion excitations in TaP.

Samples used in the present NQR study were prepared by the chemical transport method. In a first step, TaP was synthesized by direct reaction of the elements tantalum (Alfa Aesar 99.98%) and red phosphorus (Alfa Aesar 99.999%) at 500 °C and 600 °C in an evacuated fused silica tube for 72 h. Starting from this microcrystalline powder, TaP was crystallized by a chemical transport reaction (CTR) in a temperature gradient from 900 °C (source) to 1000 °C (sink) and a transport agent concentration of 13 mg/cm^3 iodine (Alfa Aesar 99.998%). Crystals obtained by the CTR method were characterized by electron-probe microanalysis and powder x-ray diffraction (for more details, see Supplemental Material [20]).

The NQR experiments were carried out with either a high-quality single crystal or powder prepared from single crystals. The NQR spectra and $1/T_1T$ were measured using a standard pulsed NMR (nuclear magnetic resonance) apparatus. The spectra were taken using the frequency sweep method under zero applied magnetic field. In order to avoid any artificial broadening, fast Fourier transformed (FFT) signals were summed across the spectrum (FFT summation) or the real part was integrated after a proper phase adjustment. Since T_1 is extremely long in TaP (typically several hundred seconds at low temperatures), we employed the progressive saturation method to measure the temperature dependence of $1/T_1T$ [28]. The recovery of nuclear magnetization was fitted to the theoretical function [29] for the magnetic relaxation in NQR lines:

$$M_n(t) = M_0[1 - (Q_1 e^{(-K_1 t/T_1)} + Q_2 e^{(-K_2 t/T_1)} + Q_3 e^{(-K_3 t/T_1)})], \quad (1)$$

where Q_n and K_n are constants depending on which NQR transition is excited and the asymmetry parameter of the electric field gradient (EFG). Using a set of principal axes, the quadrupole Hamiltonian can be written as [30]

$$H_Q = \frac{e^2qQ}{4I(2I-1)}\left[3I_z^2 - I(I+1) + \frac{1}{2}\eta(I_+^2 - I_-^2)\right], \quad (2)$$

where eq is the largest component of the EFG tensor V_{zz} and eQ is the nuclear quadrupole moment. The EFG tensor is generally defined as $|V_{zz}| \geq |V_{yy}| \geq |V_{xx}|$, with the asymmetry parameter $\eta = (V_{xx} - V_{yy})/V_{zz}$. The quadrupole-split nuclear energy levels E_m and the resultant transition frequencies can be readily calculated numerically by diagonalizing Eq. (2). For $\eta = 0$, the energy levels can simply be expressed as

$$E_m = \frac{1}{6}h\nu_Q[3m^2 - I(I+1)], \qquad \nu_Q = \frac{3e^2qQ}{h2I(I-1)}, \quad (3)$$

where ν_Q is the quadrupole coupling constant. The NQR occurs for the transition between two levels m and $m+1$, and the resonance condition can be written as $f_Q = \nu_Q(2|m|+1)/2$. Therefore, for $\eta = 0$, three NQR lines for $I = 7/2$ are expected at ν_Q, $2\nu_Q$, and $3\nu_Q$ with equal spacing.

We searched for the NQR signal in TaP powder in a frequency range from 20 to 80 MHz at 4.2 K and found three resonance lines. The observed ^{181}Ta NQR spectra at 4.2 and 40 K are shown in Figs. 1(a) and 1(b). One can immediately observe that the three lines are not equally spaced, meaning that the value of η is sizable. By fitting each line at 4.2 K to a Lorentzian, we obtained the peak frequencies $f_1 = 28.95$ MHz, $f_2 = 36.08$ MHz, and $f_3 = 56.67$ MHz. Although the full width at half maximum (FWHM) of the spectra is about 800 kHz, the line profiles are Lorentzian with long spectral tails. This implies that the EFG has a rather broad distribution. Since the Ta nuclear quadrupole moment is quite large (besides rare-earth and actinide elements, the ^{181}Ta nucleus has the second-largest Q value), the NQR spectrum can be broadened easily by merely a slight local inhomogeneity or nonstoichiometry in the composition. A least-squares fit of the observed peak frequency to the theoretical quadrupole interaction obtained from exact diagonalization gives us

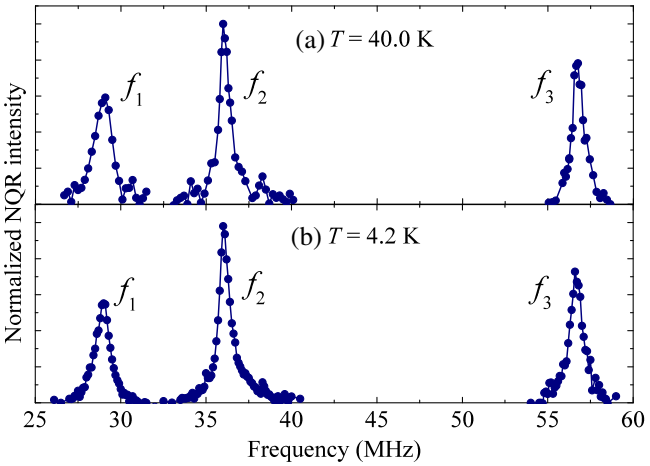

FIG. 1. Typical ^{181}Ta NQR spectra in TaP obtained from the spin-echo real part integration at 40 (a) and 4.2 K (b). The data were taken in 0.1 MHz steps across the spectrum. The lines f_1, f_2, and f_3 correspond to $\pm 3/2 \leftrightarrow \pm 1/2$, $\pm 5/2 \leftrightarrow \pm 3/2$, and $\pm 7/2 \leftrightarrow \pm 5/2$ transitions, respectively.

$\nu_Q = 19.250$ MHz and $\eta = 0.423$. The same results were also obtained for a small single crystal at 4.2 K. We also measured the spectra up to 80 K and found that there is no appreciable temperature dependence of the η value but ν_Q has a gradual decrease with increasing temperature [31] (see Supplemental Material [20] for more details).

In order to extract the quadrupole interaction in TaP theoretically, we performed band structure calculations using the density functional theory (DFT) code FPLO [32]. We used the Perdew-Wang parametrization of the local density approximation for the exchange-correlation functional [33,34]. The strong SOC in TaP is taken into account by performing full-relativistic calculations, wherein the Dirac Hamiltonian with a general potential is solved. The treatment of a finite nucleus is implemented in the code, necessary for accurate estimation of NQR parameters [35]. As a basis set, we chose Ta ($4f/5s5p6s7s8s5d6d7d6p7p5f$) and P ($2s2p3s4s5s3p4p5p3d4d4f$) semicore or valence states. The higher-lying states of the basis set are essentially important for the calculation of the EFG tensor with components $V_{ij} = \partial^2 V/\partial x_i \partial x_j$. The low-lying states were treated fully relativistically as core states. A well-converged k mesh in 1210 k points was used in the irreducible part of the Brillouin zone. Theoretically, the quadrupole coupling ν_Q can be obtained by calculating the EFG at the Ta nuclear site which is defined as the second partial derivative of the electrostatic potential $v(r)$ at the position of the nucleus $V_{ij} = [\partial_i \partial_j v(0) - \Delta\delta_{ij} v(0)/3]$. Our calculations result in $V_{xx} = -1.186 \times 10^{21}$ V/m^2, $V_{yy} = -2.354 \times 10^{21}$ V/m^2, and $V_{zz} = 3.540 \times 10^{21}$ V/m^2, where the principal axis of the EFG is [100] for one Ta atom and [010] for the second Ta atom in the unit cell. Using these values and Eq. (2), we obtained $\nu_Q = 20.057$ MHz and $\eta = 0.33$. These theoretical values are in good agreement with the experimental values, assuring that our line assignment to the quadrupole transitions is correct.

Before discussing the temperature dependence of $1/T_1T$, we have to make sure that the relaxation is governed by the magnetic fluctuations associated with the conduction electrons, although the density is quite small in semimetals. To answer this, we have made careful measurements of the time dependence of the recovery of nuclear magnetization from saturation to thermal equilibrium for all temperatures and NQR lines. Then, assuming that magnetic fluctuations are responsible for the nuclear relaxation process, the relaxation curves were fitted to Eq. (1) using calculated prefactors and exponents (Table I) for the observed value of $\eta = 0.423$. The experimental results and fitted curves are shown in Fig. 2. Here, we have a perfect match between the two for all temperatures and NQR lines, providing very strong evidence that the relaxation process is totally governed by magnetic fluctuations and yielding assurance to the accuracy of the T_1 values that were extracted. It should also be noted that there exists no impurity contribution to the relaxation process at low temperatures based on the following facts: (i) The recovery curves are governed by only one single relaxation process even in the low-temperature regime, (ii) the chemical element analysis detects no magnetic impurities (Fe, Co, Ni, Mn, Cr) in the limit of the instrumental resolution (< 10 ppm for each element), and (iii) the overall small and diamagnetic bulk susceptibility of the TaP polycrystalline NQR sample shows a rather small paramagnetic increase below 20 K which may be due to a 50 ppm level of magnetic impurities, but the electron spin resonance (ESR) could not confirm this. Therefore, we could not rule out completely the existence of a finite impurity concentration, but on that level it will not effect the NQR results presented (see Supplemental Material [20]).

TABLE I. The calculated prefactors and exponents in Eq. (1) for $\eta = 0.423$, used for the least-squares fit shown in Fig. 2.

$K_1 = 3.01028$, $K_2 = 8.7084$, $K_3 = 17.42483$			
f_1 line	$Q_1 = 0.05073$	$Q_2 = 0.45677$	$Q_3 = 0.49250$
f_2 line	$Q_1 = 0.07624$	$Q_2 = 0.02126$	$Q_3 = 0.90250$
f_3 line	$Q_1 = 0.19320$	$Q_2 = 0.51185$	$Q_3 = 0.29495$

The temperature dependence of $1/T_1T$ has been measured mainly for the f_2 line, and the obtained result is shown in Fig. 3(a). One can immediately observe that there

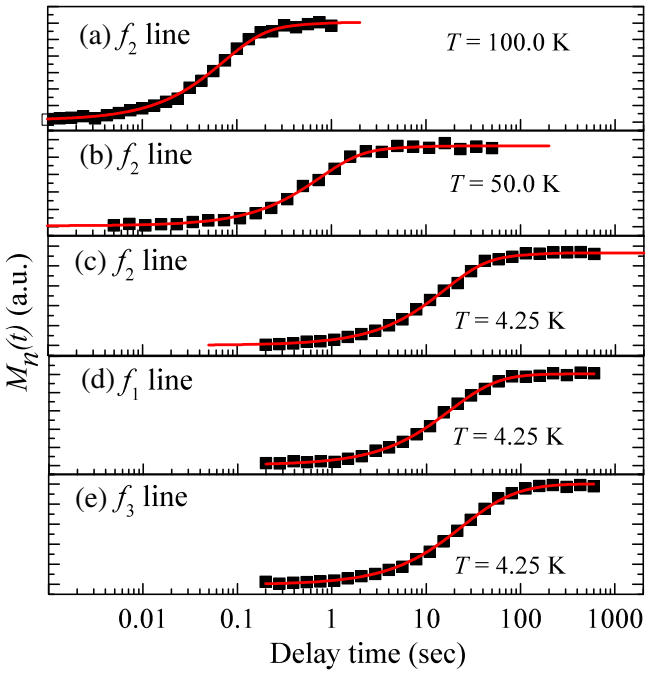

FIG. 2. Recovery of the nuclear magnetization $M_n(t)$ measured by the NQR intensity after saturation to the thermal equilibrium value for the f_2 line at 100 (a), 50 (b), and 4.25 K (c), the f_1 line at 4.25 K (d), and the f_3 line at 4.25 K (e). The red curves are the least-squares fit of the data derived using Eq. (1). The perfect fit in all cases demonstrates the fact that the relaxation is governed by magnetic fluctuations.

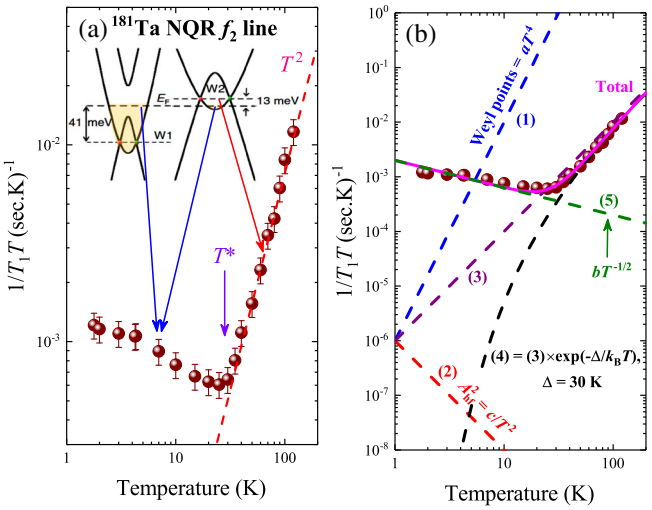

FIG. 3. (a) The temperature dependence of $1/T_1T$ of TaP along with the schematics of the band structure. At $T^* \approx 30$ K, the relaxation process crosses over between two different regimes. (b) Schematic illustration of Eq. (5): Curves (1), (2), and (3) are expected temperature dependence from the second term (Weyl nodes) not including the exponent, while curve (4) includes the exponent. The $T^{-1/2}$ dependence associated with the conventional bands is depicted by curve (5). The magenta curve is the total relaxation behavior expected from Eq. (5) and matches the experimental results.

exists a characteristic temperature $T^* \approx 30$ K, where the relaxation process has a crossover from a high-temperature T^2 behavior (which is presumably associated with the excitations in the nodal structure of Weyl points) to the low-temperature Korringa excitations [36] for parabolic bands [$E \propto k^2$ and $N(E) \propto \sqrt{E}$] with a weak temperature dependence.

Quite generally, $1/T_1T$ can be expressed using the wave-vector- (q) and frequency- (ω) dependent magnetic susceptibility $\chi(q,\omega)$, characterizing the magnetic excitations in a system as [37]

$$\frac{1}{T_1T} = \frac{2\gamma_n^2 k_B}{g^2\mu_B^2}\sum_q A_q^2 \frac{\chi''_\perp(q,\omega_n)}{\omega_n}, \tag{4}$$

where $\chi''_\perp(q,\omega)$ is the transverse component of the imaginary part of $\chi(q,\omega)$, γ_n is the nuclear gyromagnetic ratio, A_q is the q-dependent hyperfine coupling constant, and ω_n is the resonance frequency. Presently, a proper microscopic theory to accurately calculate $\chi(q,\omega)$ for multiband systems is lacking (see the discussion in Supplemental Material [20], which includes Refs. [34,38,39]). Consequently, we have evaluated a theoretical estimate for $1/T_1T$ based on a noninteracting itinerant electron approximation, using the standard DFT. In the band structure of TaP, besides the normal bands, two types of Weyl points appear. The first set of Weyl points, termed $W1$ and located in the $k_z = 0$ plane, lie ~40 meV below E_F. The second set of Weyl points, $W2$, which lie nearly in the $k_z = \pi/c$ plane (c is the lattice parameter along z) are ~13 meV above E_F [12]. This feature is shown schematically in the inset in Fig. 3(a) (see details in Supplemental Material [20]). Based on this band structure, one can easily imagine that the conventional Korringa process is valid for very low temperatures, with the upper bound limited by the energy of $W2$. Upon further increasing the temperature, excitations at the Weyl node $W2$ should become progressively dominant. Then, $1/T_1T$ may be phenomenologically expressed in a two-channel relaxation model by

$$\frac{1}{T_1T} = \frac{\pi k_B}{h}(A_p^{\rm hf})^2 N_p(E)^2 + \alpha\left[(A_W^{\rm hf})^2 \int \left\langle \frac{N_W(E)^2}{N_0^2}\right\rangle f(E)\{1-f(E)\}dE\right] \cdot \exp\left(-\frac{\Delta E}{k_BT}\right), \tag{5}$$

where the first term corresponds to excitations associated with parabolic bands ($E \propto k^2$) via the conventional Korringa process [36] with the hyperfine coupling constant $A_p^{\rm hf}$. The second term is characteristic to the excitations of the Weyl nodes and linear bands ($E \propto k$) with $A_W^{\rm hf}$. Herein, we have ignored the q dependence. α is the scaling factor. The term $N_W(E) = N_0 E/[E^2 - \Delta(\theta,\phi)]^{1/2}$ depends on the nodal structure, and $f(E)$ is the Fermi distribution function. Because of the gap (ΔE) between $W2$ and E_F, we include an activation term $\exp(-\Delta E/k_BT)$ in the second process. In general, for the point nodal case, we know $\Delta(\theta,\phi) = \Delta_0 \sin\theta$, and $N(E) \propto E^2$; accordingly, $1/T_1T \propto T^4$, which was observed experimentally for a point node superconductor [37]. Recently, anomalous hyperfine coupling due to orbital magnetism in the Weyl node has been predicted theoretically [27], where the orbital contribution to $A_W^{\rm hf}$ has a $1/T$ dependence. Then, the second term of Eq. (5) becomes $T^2\exp(-\Delta E/k_BT)$. For the first term ($T < 30$ K), experimental data show a $T^{-1/2}$ temperature dependence, despite the temperature independence of the Korringa process. The origin of this is not clear, but we may speculate that correlation among excited quasiparticles may affect it. Setting $\Delta E/k_B \approx T^*$ (30 K), the expected temperature dependence is obtained by summing up the above contributions. As schematically shown in Fig. 3(b), choosing $\alpha = 10^{-3}$, Eq. (5) is in fairly good agreement with the experiment. In particular, we clearly see a T^2 dependence for $T > T^*$ which we believe to be the manifestation of Weyl fermion excitations near the Weyl points in TaP.

In conclusion, we have reported the observation of a complete set of ^{181}Ta NQR lines in the Weyl semimetal TaP. All observed NQR lines are consistently assigned to the transitions between m and $(m+1)$ states ($m = \pm 5/2$, $\pm 3/2$, and $\pm 1/2$). From our measurements, we obtain an asymmetry parameter $\eta = 0.423$ and a quadrupole coupling constant of $\nu_Q = 19.250$ MHz. These findings are in

good agreement with DFT calculations, which provide $\eta = 0.33$ and $\nu_Q = 20.057$ MHz. The low-energy excitations as a function of the temperature were probed through the Ta spin-lattice relaxation rate $(1/T_1T)$, which shows a pronounced T^2 behavior above $T^* = 30$ K and a $T^{-1/2}$ behavior below T^*. The relaxation process below T^* is mostly related to the conventional density of states $[N(E) \propto \sqrt{E}]$, which yields an almost constant density of states at E_F (Korringa process). However, we have to postulate correlation effects as an origin for the $T^{-1/2}$ behavior below T^*. For $T > T^*$, by taking into account temperature-dependent orbital hyperfine coupling and activation-type relaxation processes to the $W2$ points, we were able to explain the T^2 behavior in a convincing way. For the unique case of the Ta-based WSM, we have shown that the NQR method is a direct local probe for low-energy Weyl fermion excitations in the bulk. This is rather important, because such excitations are one of the main ingredients for the unconventional electron transport found in these new materials. It would be interesting to take a deeper look into other conventional bulk probes such as thermopower to explore signatures of Weyl fermions and to extend the NQR study to other Ta-based Weyl and Dirac semimetals.

We thank B. Dóra for discussions and critical reading of the manuscript. Discussions with H. Harima, K. Kanoda, M. Majumder, and E. Hassinger are also appreciated. We thank U. Schmidt and G. Auffermann for the chemical analysis of the TaP crystals and J. Sichelschmidt for temporary ESR measurements. T. K., Y. K., and H. T. appreciate the financial support from JSPS KAKENHI Grants (No. 15K21732 and No. 15H05885). D. K. acknowledges funding via FOR 1346 from the Deutsche Forschungsgemeinschaft.

*Michael.Baenitz@cpfs.mpg.de

[1] A. H. Castro Neto, F. Guinea, N. M. R. Peres, K. Novoselov, and A. Geim, Rev. Mod. Phys. **81**, 109 (2009).
[2] C. L. Kane and E. J. Mele, Phys. Rev. Lett. **95**, 146802 (2005).
[3] B. A. Bernevig, T. L. Hughes, and S. C. Zhang, Science **314**, 1757 (2006).
[4] M. Z. Hasan and C. L. Kane, Rev. Mod. Phys. **82**, 3045 (2010).
[5] T. O. Wehling, A. M. Black-Schaffer, and A. V. Balatsky, Adv. Phys. **63**, 1 (2014).
[6] S. M. Young, S. Zaheer, J. C. Y. Teo, C. L. Kane, E. J. Mele, and A. M. Rappe, Phys. Rev. Lett. **108**, 140405 (2012).
[7] Z. Wang, H. Weng, Q. Wu, X. Dai, and Z. Fang, Phys. Rev. B **88**, 125427 (2013).
[8] H. Weng, C. Fang, Z. Fang, B. A. Bernevig, and X. Dai, Phys. Rev. X **5**, 011029 (2015).
[9] C. Shekhar, A. K. Nayak, Y. Sun, M. Schmidt, M. Nicklas, I. Leermakers, U. Zeitler, Y. Skourski, J. Wosnitza, Z. Liu, Y. Chen, W. Schnelle, H. Borrmann, Y. Grin, C. Felser, and B. Yan, Nat. Phys. **11**, 645 (2015).
[10] Y. Sun, S.-C. Wu, and B. Yan, Phys. Rev. B **92**, 115428 (2015).
[11] S.-Y. Xu *et al.*, Sci. Adv. **1**, e1501092 (2015).
[12] F. Arnold, C. Shekhar, S.-C. Wu, Y. Sun, R. D. dos Reis, N. Kumar, M. Naumann, M. O. Ajeesh, M. Schmidt, A. G. Grushin, J. H. Bardarson, M. Baenitz, D. Sokolov, H. Borrmann, M. Nicklas, C. Felser, E. Hassinger, and B. Yan, Nat. Commun. **7**, 11615 (2016).
[13] N. Curro, in *Encyclopedia of Magnetic Resonance* (Wiley, New York, 2011).
[14] N. J. Curro, Rep. Prog. Phys. **72**, 026502 (2009).
[15] R. E. Walstedt, *Springer Tracts in Modern Physics* Vol. 228 (Springer-Verlag, Berlin, 2008).
[16] Y. Kuramoto and Y. Kitaoka, *Dynamics of Heavy Electrons* (Oxford University, New York, 2000).
[17] G. Aeppli and Z. Fisk, Comments Condens. Matter Phys. **16**, 155 (1992); P. Riseborough, Adv. Phys. **49**, 257 (2000).
[18] T. Caldwell, A. P. Reyes, W. G. Moulton, P. L. Kuhns, M. J. R. Hoch, P. Schlottmann, and Z. Fisk, Phys. Rev. B **75**, 075106 (2007).
[19] E. M. Brüning, M. Brando, M. Baenitz, A. Bentien, A. M. Strydom, R. E. Walstedt, and F. Steglich, Phys. Rev. B **82**, 125115 (2010).
[20] See Supplemental Material at http://link.aps.org/supplemental/10.1103/PhysRevLett.118.236403 for more measurement details.
[21] G. C. Carter, L. H. Bennett, and D. J. Kahan, *Metallic Shifts in NMR*, Progress in Materials Science (Pergamon, New York, 1977).
[22] S. Mukhopadhyay, S. Krämer, H. Mayaffre, H. F. Legg, M. Orlita, C. Berthier, M. Horvatić, G. Martinez, M. Potemski, B. A. Piot, A. Materna, G. Strzelecka, and A. Hruban, Phys. Rev. B **91**, 081105(R) (2015).
[23] X. Zhang, Z. Hou, Y. Wang, G. Xu, C. Shi, E. Liu, X. Xi, W. Wang, G. Wu, and X.-x. Zhang, Sci. Rep. **6**, 23172 (2016).
[24] B. Nowak and D. Kaczorowski, J. Phys. Chem. C **120**, 21797 (2016).
[25] M. Naito, H. Nishihara, and S. Tanaka, J. Phys. Soc. Jpn. **53**, 1610 (1984).
[26] S. Wada and K. Asayama, J. Phys. Soc. Jpn. **34**, 1168 (1973).
[27] Z. Okvátovity, F. Simon, and B. Dóra, Phys. Rev. B **94**, 245141 (2016).
[28] V. F. Mitrović, E. E. Sigmund, and W. P. Halperin, Phys. Rev. B **64**, 024520 (2001).
[29] J. Chepin and J. H. Ross, J. Phys. Condens. Matter **3**, 8103 (1991).
[30] A. Abragam, *The Principle of Nuclear Magnetism* (Clarendon, Oxford, 1961); C. P. Slichter, *Principles of Magnetic Resonance* (Springer, New York, 1989).
[31] J. Christiansen, P. Heubes, R. Keitel, W. Klinger, W. Loeffler, W. Sandner, and W. Witthuhn, Z. Phys. B **24**, 177 (1976).
[32] K. Koepernik and H. Eschrig, Phys. Rev. B **59**, 1743 (1999).
[33] J. P. Perdew and Y. Wang, Phys. Rev. B **45**, 13244 (1992).
[34] A. A. Mosto, J. R. Yates, Y. S. Lee, I. Souza, D. Vanderbilt, and N. Marzari, Comput. Phys. Commun. **178**, 685 (2008).

[35] K. Koch, K. Koepernik, D. Van Neck, H. Rosner, and S. Cottenier, Phys. Rev. A **81**, 032507 (2010).
[36] J. Korringa, Physica (Utrecht) **16**, 601 (1950).
[37] K. Katayama, S. Kawasaki, M. Nishiyama, H. Sugawara, D. Kikuchi, H. Sato, and G. Q. Zheng, J. Phys. Soc. Jpn. **76**, 023701 (2007).
[38] J. P. Perdew, K. Burke, and M. Ernzerhof, Phys. Rev. Lett. **77**, 3865 (1996).
[39] H. Michihiro, K. Ishikawa, K. Miyagawa, M. Tamura, C. Berthier, D. Basko, A. Kobayashi, G. Matsuno, and K. Kanoda, Nat. Commun. **7**, 12666 (2016).